

Final-Year Practical Project Cover Sheet

Students: Please fill in and use it as the front page of your project report

Name of Student: Yixuan Li

CID: 02254979

Degree Stream: Biological Science

Date: 5th June 2025

Word Count: 5998

Project Title: An agent-based model of natural killer cell-tumour cell interaction

I hereby declare that this Project has not been submitted, either in the same or different forms, to this or any other university for a degree. I also declare that this Project does not draw from any other work prepared under consultancy or other professional undertaking, by myself or jointly with other authors in any way other than that duly and explicitly acknowledged herewith.

Name of Supervisor: Dr Ruben Perez-Carrasco

Name of Examiner 1: Dr Giovanni Sena

Name of Examiner 2: Prof Robert Endres

Final-Year Practical Project reports: assessment criteria

These criteria are to be used for all types of final-year practical project report: *Lab project, Field project and Computational project*. Outside reading is fundamental when writing up a research project, so is not mentioned explicitly in the criteria that follow. Most outside reading should be from the peer-reviewed scientific literature, including primary research papers. The expected format of the report is described in detail in the guidelines for **Practical project reports**.

Class	%	Criteria
1 st	100	Report is of sufficient quality to submit for publication to an international peer-reviewed journal (assuming, ideally, that positive and negative results have equal merit).
	95	Report is close to a publishable standard, containing a succinct survey of the most important primary literature and an accurate and logical account and justification of the methods used . It presents the results in a publishable format , and knowledgeably applies any necessary mathematical and/or statistical techniques . Discussion of results demonstrates high levels of rigour and critical ability in the context of the relevant literature. Report demonstrates an appreciation of the limitations of the experimental or other procedures, shows attention to detail (in references, figures, etc.), and shows clear and possibly novel insight into the subject.
	90	
	85	Excellent report, meeting all of the criteria for a mark of 68 and most but not all of the criteria for a mark of 90+ .
	80	
	76	Excellent report, meeting all the criteria for a mark of 68 and one or a few of the criteria for a mark of 90+ .
	72	
2A	68	Very good, well-structured report written in good scientific style (i.e. in clear, concise, direct, precise, dispassionate scientific English, including all important details). It shows the following features: (i) an ability to carry out experimental procedures successfully to generate original results (which may be negative and need not be novel); (ii) a very good understanding of the study design and the methods used to generate and analyse the data; (iii) appropriate – if not high-level – analyses ; (iv) clear presentation of results ; (v) sound knowledge of how the study fits in to the relevant literature ; (vi) some critical interpretation of the results and the study overall.
	65	
	62	
2B	58	Good report showing the following features: (i) an ability to follow experimental procedures ; (ii) basic understanding of the relevant concepts and methods ; (iii) mostly logical structure and scientific style ; (iv) reasonable interpretation of the data or information collected; and (iv) a reasonable attempt to relate the results to the latest literature .
	55	
	52	Reports that are too long, poorly written , and/or that show poor use of references are unlikely to be marked above a 2B.
3 rd	48	Acceptable report showing the following features: (i) an ability to follow some experimental procedures ; (ii) a weak grasp of most of the relevant concepts and methods ; (iii) need for close guidance in design and interpretation ; and (iv) at best limited relation of the results to the relevant literature . Research projects in this bracket are likely to be marred by significant errors, important omissions, brevity and/or a failure to interpret the data critically.
	45	
	42	
Fail	38	Poor report showing the following features: (i) understanding of less than half of the theoretical basis of the project ; (ii) evidence of widespread difficulty following procedures to generate and analyse data; (iii) need for complete instruction in design and interpretation ; (iv) does not relate the outcome of the experimental work to the literature .
	35	
	30	
	25	Report contains more than a few relevant sentences but shows very little understanding of the background to the project, the project design, or the methods used to generate or analyse the data. Students in this bracket are unlikely to have been able to carry out even basic procedures, despite proper instruction.
	20	
	15	Report contains only a few sentences relevant to the subject , and does not contain any interpretable results.
	10	
	5	
	0	Report contains nothing relevant or was not submitted.

Practical and Literature Projects: Supervisor assessment criteria for lab/data/field-work or research proposal development

Supervisors are required to provide a **single mark that reflects all aspects of a student's performance** when assessed against the marking criteria. This mark may take into account aspects of the final report as it affects assessment of overall performance, but independent assessment and provision of a mark for the final report are not required.

Class	%	Criteria
1 st	100	Student worked safely, confidently, diligently, and designed appropriate investigations (lab and/or literature) . Where applicable, the student developed a high level of technical expertise . Student kept supervisor informed of progress, but consistently showed originality and initiative , and did not require any close management. Student contributed strongly to the research in the lab/field or in developing the research proposal . Throughout the project the student demonstrated a high level of rigour and critical, synthetic and/or analytical ability in the context of the relevant literature and an appreciation of the strengths and limitations of the study design or research project development . Overall, the student performed like a research postgraduate.
	95	
	90	
	85	Student met all of the criteria for a mark of 68 as well as most of the criteria for a mark of 90+
	80	
	76	Student met all of the criteria for a mark of 68 as well as one or a few of the criteria for a mark of 90+ .
2A	72	
	68	Student's lab or field work and research proposal development was performed competently . The student contributed significantly to the experimental and/or research proposal design , worked with some diligence, largely independently , and where applicable learned procedures well.
	65	
2B	62	The student shows a very good understanding of the study design and the methods used to generate and analyse the data or those proposed as part of a research proposal; they demonstrated sound knowledge of how the study/proposed study fits in to the relevant literature ; and shows some rigour and critical, synthetic or analytical ability in the context of the relevant literature and an appreciation of some of the strengths and/or limitations of the study design or research project development
	58	Student's lab, field and/or research proposal development work was performed safely throughout . The student had some input into experimental design and/or research proposal design and worked with some diligence . The student was able to work usefully, requiring only day-to-day supervision .
	55	
3 rd	52	The student shows basic understanding of the relevant concepts and methods and a reasonable ability to place the material in the context of the relevant literature, but only a partial appreciation of the strengths or limitations of the study design or research project development .
	48	Student showed some ability to follow experimental procedures, or to do some research proposal development work, without close supervision and appreciated safety aspects , but the work was limited in quantity or quality . Student's input into experimental design and/or research proposal design was minimal . Student performance in this class is likely to be marred by errors of understanding, and a failure to appreciate the strengths or limitations of the study design or research project development .
	45	
Fail	42	
	38	Student worked for up to a half of the expected time and worked safely/adequately in the field, lab and/or on the research proposal only when closely supervised . Student showed very little or no initiative or independence .
	35	
Fail	30	Student performance in this class is likely to be marred by significant errors of understanding, and a failure to appreciate the limitations of the study design or research project development .
	25	Student attended the laboratory or field site, or meetings with supervisor(s), for up to a third of the expected time and performed some work safely/adequately but only when closely managed . Very little useful work completed in field, lab and/or research proposal .
	20	
	15	Student attended the laboratory or field site, or meetings with supervisor(s) but either attended for less than a quarter of the expected time or worked in an unsafe or otherwise wholly unsatisfactory fashion despite instruction. Negligible amount of work completed in the field, lab and/or on the research proposal.
	10	
	5	
Fail	0	Student did not attend the laboratory or field site, or meetings with supervisor(s), or was barred for preventable reasons (e.g., an unacceptable attitude to safety or to the work in general) or failed to generate a research proposal.

IMPERIAL

IMPERIAL COLLEGE LONDON

DEPARTMENT OF LIFE SCIENCE

An Agent-Based Model of Natural Killer Cell-Tumour Cell Interaction

Author:

Yixuan Li

CID:

02254979

Supervisor:

Dr. Ruben Perez-Carrasco

Day-to-Day Supervisor:

Elephes Sung

Contents

Abstract	5
Chapter 1 Introduction.....	6
Chapter 2 Methods	11
2.1 Model construction	11
2.1.1 Stochastic Cell Motility	11
2.1.2 NK Cell Killing Probability and Spatial heterogeneity	14
2.1.3 Tumour Death Factor Dynamics.....	16
2.2 Statistical analysis	18
Chapter 3 Results	19
3.1 Manipulating Cell Motility Parameters	22
3.1.1 Impacts of cell motility in cell trajectories	22
3.1.2 Impacts of cell motility on NK killing outcomes	24
3.2 Impacts of E:T ratio on NK killing outcomes	27
3.3 Effects of death factor threshold on NK killing outcomes	31
Chapter 4 Discussion.....	32
Reference.....	37
Acknowledgements	42

Abstract

NK cells are emerging as a focus in cancer immunotherapy which could be made available as a safe off-the-shelf product. However, mechanisms of stochastic killing behaviour, switching between killing and non-killing outcomes at different contacts with tumour cells, exhibited by a small group of NK cells remain poorly understood. This stochasticity was hypothesised based on two primary mechanisms: (1) heterogeneous spatial distribution of receptors and ligands, coupled with variability in geometric configuration of NK cell-tumour contacts; and (2) stochastic motion of cells as well as heterogeneity of tumour sensitivity and NK cell activation status. Given the complexity of immunological systems, a computational agent-based model incorporating polarity-driven motility, NK killing probability, cell-cell physical interactions and ordinary differential equations for simulating tumour cell recovery mechanism was developed to model interactions between NK and tumour cells based on the mechanisms hypothesised. Based on the simulations, the model showed the ability to capture the stochastic killing behaviour performed by NK cells and therefore was used to explore various parameters affecting NK cell cytotoxic outcomes. It also highlights the importance of cell motility in shaping NK-tumour cell interaction and NK cytotoxic response and suggests a sufficient E:T ratio (5:1) for effective NK cell killing under certain condition. Future study will focus on validating the model and refining its predictivity.

Chapter 1 Introduction

Autologous chimeric antigen receptor engineered T-cell (CAR-T) therapy has revolutionised treatments for hematological malignancies over past decade (Goyco Vera et al., 2024). Despite its success, high-cost and time-consuming manufacturing of personalised CAR-T therapy limits patient access (Borgert, 2021), making an off-the-shelf CAR-T cells desirable. However, allogenic T-cells carry high risk of graft-versus-host disease (GVHD) mediated by T-cell receptor (TCR). Although this risk can be mitigated by gene editing to remove TCR, this complicates manufacturing process and introduces an unclear safety profile (Mailankody et al., 2023). Natural killer (NK) cell therapy is considered as an alternative of allogenic CAR-T therapy. NK cells are innate lymphocytes that perform cytotoxic functions to tumour cells in a non-antigen specific manner (Wolf, Kissiov and Raulet, 2023). Since NK cells do not express TCR, allogenic NK cells lack the potential to cause GVHD and could be made available as a safe off-the-shelf product for immediate clinical use (Liu et al., 2020). Therefore, NK cells are emerging as a focus in cancer immunotherapy.

NK cells are equipped with an array of activating and inhibitory receptors. For example, natural killer group 2 member D protein (NKG2D) receptor is the activating receptor that expressed on almost all NK cells (Raulet, 2003). Inhibitory Killer Ig-like Receptors (KIR) are a major group of inhibitory receptors, which inhibits the killing when encountering normal cells expressing human leukocyte antigen (HLA) class I molecules, called self-tolerance (Pende et al., 2019). Receptors trigger signal cascades when binding to activating and inhibitory ligands at immunological synapse. NK cells make killing decision based on the integration and balance of activating and inhibitory signals transmitted by various NK cell surface receptor. If activating signals outweigh inhibitory signals, NK-mediated

cytotoxicity involving cytotoxic degranulation containing perforin and granzymes as well as death ligands-induced apoptosis happen (Wolf, Kissiov and Raulet, 2023). Although several aspects of NK cell immune responses are understood, recent observations have revealed unexpected phenomena related to their cytotoxic activity. A study using microchip-based, time-lapse imaging analysis classified NK cells into five distinct classes based on heterogeneity of cytotoxic responses and observed that minority of NK cells was responsible for majority of tumour cell deaths, potentially constraining cytotoxic efficacy (Figure 1A). Notably, a small group of NK cells exhibited stochastic killing, switching between killing and non-killing outcomes at different tumour contacts (Vanherberghen et al., 2013), see Figure 1B. NK cells were reported having the variegated expression of activating and inhibitory receptors within individual (Horowitz et al., 2013). The expression level of activating receptors, e.g., NKG2D expression on NK cell correlates with the cytotoxic outcomes (Konjević et al., 2009). This finding may explain the presence of killing and non-killing outcomes but cannot account for the switch between them, suggesting that population-level expression heterogeneity alone is insufficient to explain the stochastic killing behaviour. Although many research investigated on cytotoxic responses on NK cells (Guldevall et al., 2016; Subedi et al., 2021), few studies have explored mechanisms behind diverse NK cell cytotoxic behaviors, with most focusing on serial killers—a small subset capable of delivering multiple hits consecutively (Srpan et al., 2018). No study has specifically focused on the mechanisms of stochastic killing behaviour. It remains unclear whether serial killers are fundamentally different from stochastic killing NK cells or simply more fortunate in their encounters. Understanding this is crucial for improving efficacy of NK-based immunotherapies.

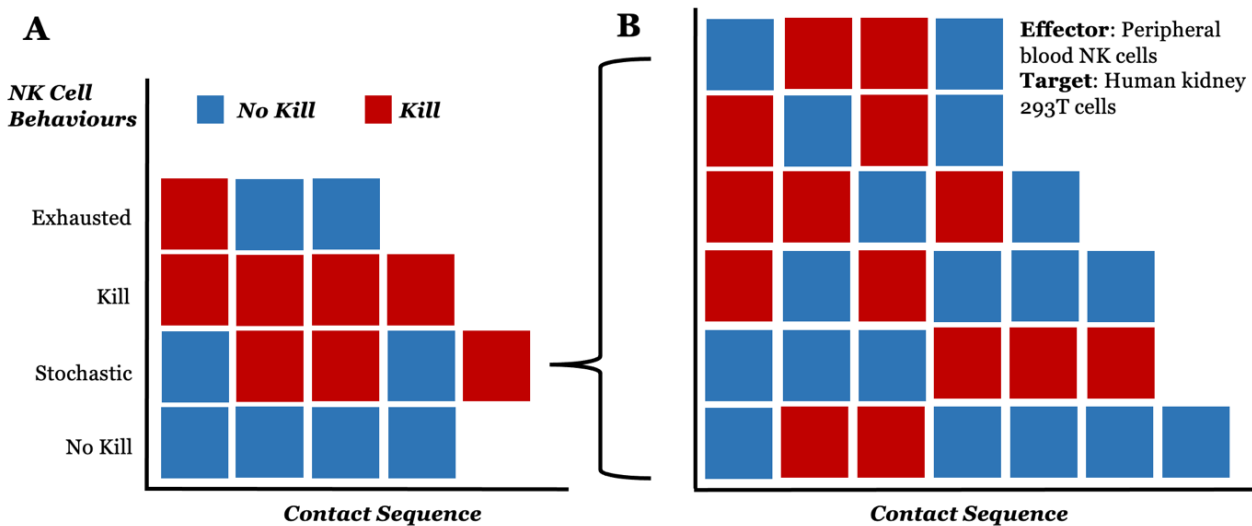


Figure 1. NK cell mediated cytotoxicity: observations. (A) The schematic of contact history for five distinct classes of NK cell cytotoxic responses, including a class of NK cells that do not have interactions (Not shown on plot). Each row represents a class of NK cell and its contact sequence. (B) The contact history of NK cells exhibiting stochastic killing behaviours. Data from Vanherberghen et al. (2013), which investigated the interaction between human kidney 293T cells and human peripheral blood NK cells. Each row represents a contact sequence observed.

To address this question, different hypotheses for mechanisms of stochastic killing behaviour were developed based on previous studies. The lateral segregation of membrane proteins compartmentalises surface receptors and ligands into microdomain, which are therefore not uniformly distributed (Lingwood and Simons, 2010). Moreover, NK cell cytotoxicity is suggested to be controlled by activating ligands distribution on target cell membrane, e.g., NKG2D ligand ULBP1 (Martinez et al., 2011), and CD16 ligands (Verron et al., 2021). Given the above, a prior unpublished thesis proposed that spatial receptors-ligands distribution along with the variability at NK cell-tumour contact sites may be the primary factors contributing to the stochastic NK cell killing behaviours (Elephes Sung, 2024), see Figure 2A. Additionally, expression level of activating receptors of NK cell was observed to positively correlated with NK cell cytotoxicity (Konjević et al., 2009).

Combining with the finding that cytotoxic T lymphocytes (CTLs) mediated apoptosis could

be countered by tumor cell intrinsic repair mechanism where CTLs and NK cell shared similar cytotoxic mechanisms (Ritter et al., 2022). Tumour cells may exhibit similar recovery mechanism in response to NK cell. Overall, the hypothesis that the stochastic motion of cells, heterogeneity of tumour sensitivity and NK cell activation status could affect the killing outcomes was proposed (Elephes Sung, 2024), see Figure 2B. In this report, these hypotheses are revisited.

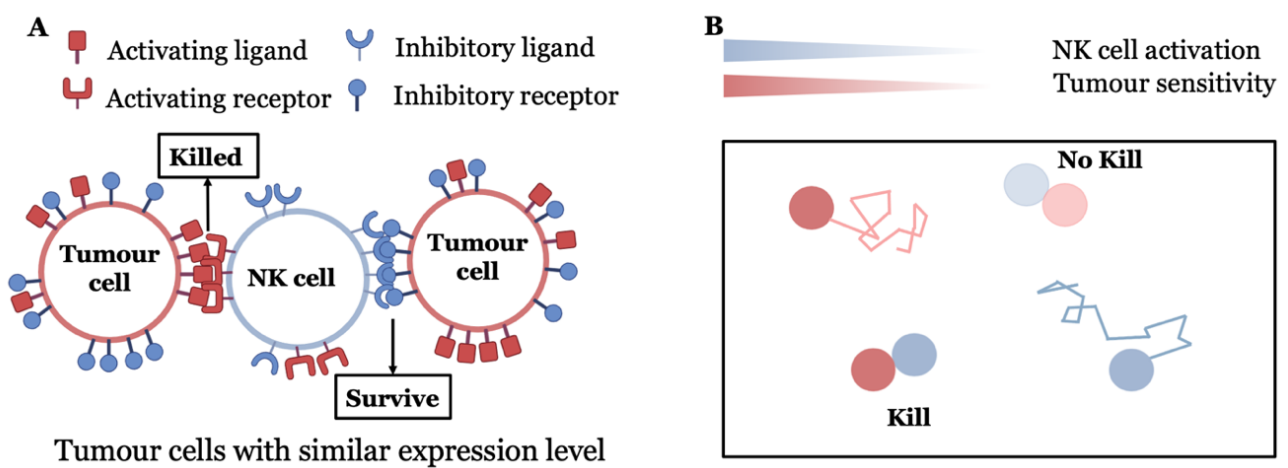


Figure 2. Stochastic killing behaviours of NK cells: hypothesis. (A) Schematic of hypothesis that heterogeneity of spatial distribution of receptors and ligands along with the variability of NK-tumour cells contact sites contributes to stochastic killing of NK cells. (B) Schematic of hypothesis that stochastic motion, heterogeneity of NK cell activation status and tumour cell sensitivity affects the killing outcomes. Adapted from unpublished thesis from Elephes Sung (2024).

As mentioned above, NK-mediated cytotoxicity outcomes are determined by many interacting components, which are extremely complex. Even though microfluidic platforms allow observation of the single-cell level dynamic (Subedi et al., 2021) and super-resolution fluorescence microscopy could image the spatial distributions on single cell (Hu, Cang and Lillemoier, 2016), it is still challenging to dissect the influence of molecular pattern on killing outcomes from other components. To explore these hypotheses, mathematical model should be developed. Given the demand to account for cell-to-cell heterogeneity in

NK cell, agent-based models (ABMs) are more suitable than the models that treat sample as homogeneous individuals (Handel, La Gruta and Thomas, 2020). ABMs model system as autonomous individuals, each making decision based on predefined rules (Bonabeau, 2002). They capture dynamic individual behaviours and interactions, making them widely used for studying immunological system. For instance, a computational multiscale agent-based model was developed to simulate spatiotemporal tumour immune response to PD1 and PDL1 inhibition (Gong et al., 2017). Notably, many studies used hybrid, multiscale model where AMB serves as scaffold to interface with mechanistic models such as ordinary differential equation (ODE) or stochastic differential equation (SDE) to simulate the dynamics (Cess and Finley, 2020; Mallet and De Pillis, 2006), making the model more powerful. Besides, Cellular Potts model (CPM), a subtype of AMB, was implemented to simulate the NK-tumour interaction (Elephes Sung, 2024). While CPM captures changes of cell morphology and cell sizes, it is computationally expensive and time-consuming. This study developed a simplified hybrid ABM that avoids the complexity of the cellular Potts model (CPM) while still capturing essential multiscale behavior efficiently.

In this report, a hybrid ABM simulating NK cell-mediated cytotoxicity was constructed based on the mechanisms previously hypothesised. This model incorporates the stochastic cell motility, tumour recovery mechanism and NK cell activation status and aims to capture the NK stochastic killing behaviours. By systematically manipulating the parameters controlling cell motility, effector-to-target ratio (E:T), cell density etc., the impacts of these parameters on NK cell killing behaviours are examined, which could provide better understanding on NK cell-mediated cytotoxicity that potentially directs and enhances design of NK cell-based immunotherapy strategy.

Chapter 2 Methods

2.1 Model construction

The basis of model is adapted from the unpublished thesis (Elephes Sung, 2024). To stimulate the NK-tumour interaction *in silico*, the stochastic motility simulated by SDE, NK cell activation status representing by NK killing probability and tumour death factor dynamics by implementing ODE are incorporated in the ABM. Each digital NK cell is assigned an initial killing probability and each tumour is assigned an initial death factor from a uniform distribution within a defined range. Simulations are conducted in two-dimensional (2D) space measuring $600 \mu m$ on each side, domain length L . Cells are initially distributed uniformly within this domain. The periodic boundary condition (PBC) was implemented, allowing cells move out of a boundary to re-enter through the opposite boundary. PBC ensures cell behaviours are not biased due to the finite size of simulation box.

2.1.1 Stochastic Cell Motility

A mathematical framework based on Ornstein-Uhlenbeck (OU) stochastic process was applied to simulate 2D stochastic cell motility (Uhlenbeck and Ornstein, 1930). A 2D vector $\vec{\mu}(t)$ representing cell polarity at time t is assigned to every cell. The following SDE captures the dynamics of polarity change over time:

$$\frac{d\vec{\mu}(t)}{dt} = -\gamma\vec{\mu}(t) + \vec{\eta}_\mu \quad (Eq. 1)$$

$-\gamma\vec{\mu}(t)$ denotes the effect driving cell polarity towards zero. Higher γ leads to faster restoration to zero. $\vec{\eta}$ denotes the white noise which keeps cell polarity away from zero. Eq.1 is implemented numerically through Euler-Maruyama algorithm:

$$\vec{\mu}(t + dt) = \vec{\mu}(t) - \gamma\vec{\mu}(t) \cdot dt + g\sqrt{dt}\vec{\epsilon}(t) \quad (Eq. 2)$$

where $\vec{\epsilon}(t)$ are independent standard normal random variables, with an intensity of g . The cell velocity is driven by the cell polarity and noise:

$$\frac{d\vec{r}(t)}{dt} = \beta\vec{\mu}(t) + \vec{\eta}_r \quad (Eq. 3)$$

where $\vec{r}(t)$ is cell position vector and $\vec{\eta}_r$ denotes the white noise. To make cell motility biophysically realistic, mechanical interactions between cells are added to describe the cell motility. The pairwise intermolecular force called Lennard-Jones (LJ) force, derived from Lenard-Jones potential calculated based on distance between cells (Jones and Chapman, 1924), is applied:

$$\vec{F}_{LJ}(\vec{r}) = 24\epsilon \left[\frac{2\sigma^{12}}{r^{13}} - \frac{\sigma^6}{r^7} \right] \hat{r} \quad (Eq. 4)$$

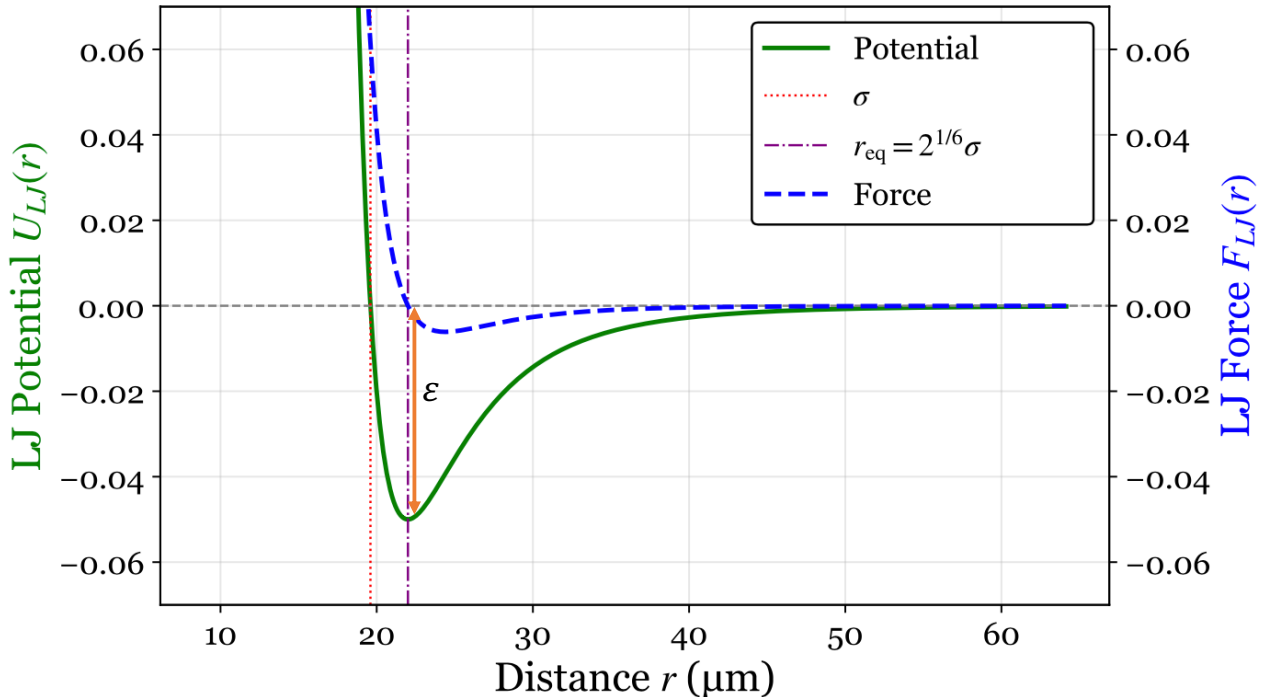


Figure 3. The Lennard-Jones potential and LJ force. LJ potential is plotted in green solid line and LJ force is plotted in blue dash line. Purple line indicates the distance

$r = 2^{\frac{1}{6}}\sigma$ where shows the minimum potential (zero force). Red line indicates the value of σ . Orange arrow refers interaction strength, ε .

Parameter ε denotes interaction strength and r denotes distances between two cells. \hat{r} gives direction of force. σ controls the interaction distance of the potential. Assuming potential is minimum ($r = 2^{\frac{1}{6}}\sigma$) — and thus stable equilibrium — occurs when two cells are just in contact (i.e., their center-to-center distance equals the sum of their cell radii), three σ values where $\sigma = \frac{\text{Sum of cell radii}}{2^{\frac{1}{6}}}$ are calculated (Figure 3). σ for tumour-tumour interaction is $21.38 \mu\text{m}$, NK-tumour interaction is $19.60 \mu\text{m}$, NK-NK interaction is $17.82 \mu\text{m}$, given NK and tumour cell radii of $10 \mu\text{m}$ and $12 \mu\text{m}$, respectively. Each neighboring cell exert force on a given cell. Combining polarity-driven motility equation (Eq.3) with the total interaction force from all neighbours (Eq.4), the final cell velocity is obtained:

$$\frac{d\vec{r}(t)}{dt} = \beta\vec{\mu}(t) + \vec{\eta}_r + \frac{1}{\lambda} \sum \vec{F}_{LJ}(t) \quad (\text{Eq. 5})$$

where an overdamped regime is assumed that the mass of cells is much smaller than its friction:

$$\vec{F} = \lambda \frac{d\vec{r}(t)}{dt} \quad (\text{Eq. 6})$$

λ denotes friction coefficient. The resulting force depends on the ration of ε and λ .

Parameter λ can be set to 1 and therefore the effect of resulting force is controlled by ε . Eq.5 is implemented numerically through Euler-Maruyama algorithm:

$$\vec{r}(t + dt) = \vec{r}(t) + \beta\vec{\mu}(t) \cdot dt + \frac{1}{\lambda} \sum \vec{F}_{LJ}(t) \cdot dt + b\sqrt{dt}\vec{\xi}(t) \quad (\text{Eq. 7})$$

Parameter $\vec{\xi}$ refers to the white noise with components that are independent standard normal random variables and has an intensity of b .

The adaptive timestep is implemented to avoid extremely large forces applied on cells due the high-level of overlaps between cells at a single timestep. The interval time Δt is defined based on the maximum forces F_{max} applied to the cells rather than a constant at each step:

$$\Delta x_{max} = F_{max} \cdot \frac{1}{\lambda} \cdot \Delta t$$

$$\Delta t = \frac{\Delta x_{max}}{F_{max}} \cdot \lambda \quad (Eq. 8)$$

where λ denotes the friction coefficient and is set to 1. The maximum displacement of cells, Δx_{max} is defined as $5 \mu m$ for each timestep. Total force F for each cell q equals to the sum of Lennard-Jones force and the polarity-driven motion at current step, derived from Eq.6:

$$F_q = \lambda \frac{d\vec{r}(t)}{dt} = \lambda \beta \vec{\mu}(t) + \lambda \vec{\eta}_r + \sum \vec{F}_{LJ}(t) \quad (Eq. 9)$$

F_{max} is the maximum total force F_q among all total forces applied on cells at current step and used to calculate the interval time Δt . If Δt is smaller than the initial timestep $1/20$ hours, Δt is applied for updating the step. Otherwise, initial timestep is used.

2.1.2 NK Cell Killing Probability and Spatial heterogeneity

NK killing probability, $P_{killing}$, is related with expression level of activating and inhibitory receptor. High killing probability indicates high activation status. Each NK cell i is randomly assigned a killing probability constant $P_{killing,i} \in [0.55, 0.6]$ from a uniform distribution. Interaction between NK cell and tumour cell starts when their distance is less than or equal to the sum of their radii ($22 \mu m$). At each NK-tumour cell contact, a killing decision (K_i) is made by performing a Bernoulli trial:

$$K_i(t) = \begin{cases} 1, & \text{if } v < P_{killing,i} \\ 0, & \text{otherwise} \end{cases} \quad \text{where } v \sim U(0,1) \quad (Eq. 10)$$

The contact checking, v is drawn from a uniform distribution $U(0, 1)$ and compare with killing probability specific for each NK cell. If v is smaller than $P_{killing}$, NK cell initiates

killing behaviour, where $K_i(t) = 1$. If not, tumour cell survives and death factor starts to decrease ($K_i(t) = 0$), see Figure 4A. After each contact, $P_{killing}$ will decrease by 0.02 due to NK cell exhaustion. This algorithm reflects both activation status of NK cell and randomness of local receptors-ligands distribution encountered at immunological synapse. It is a reductionist approach that abstracts variability of molecular patterns at contact site

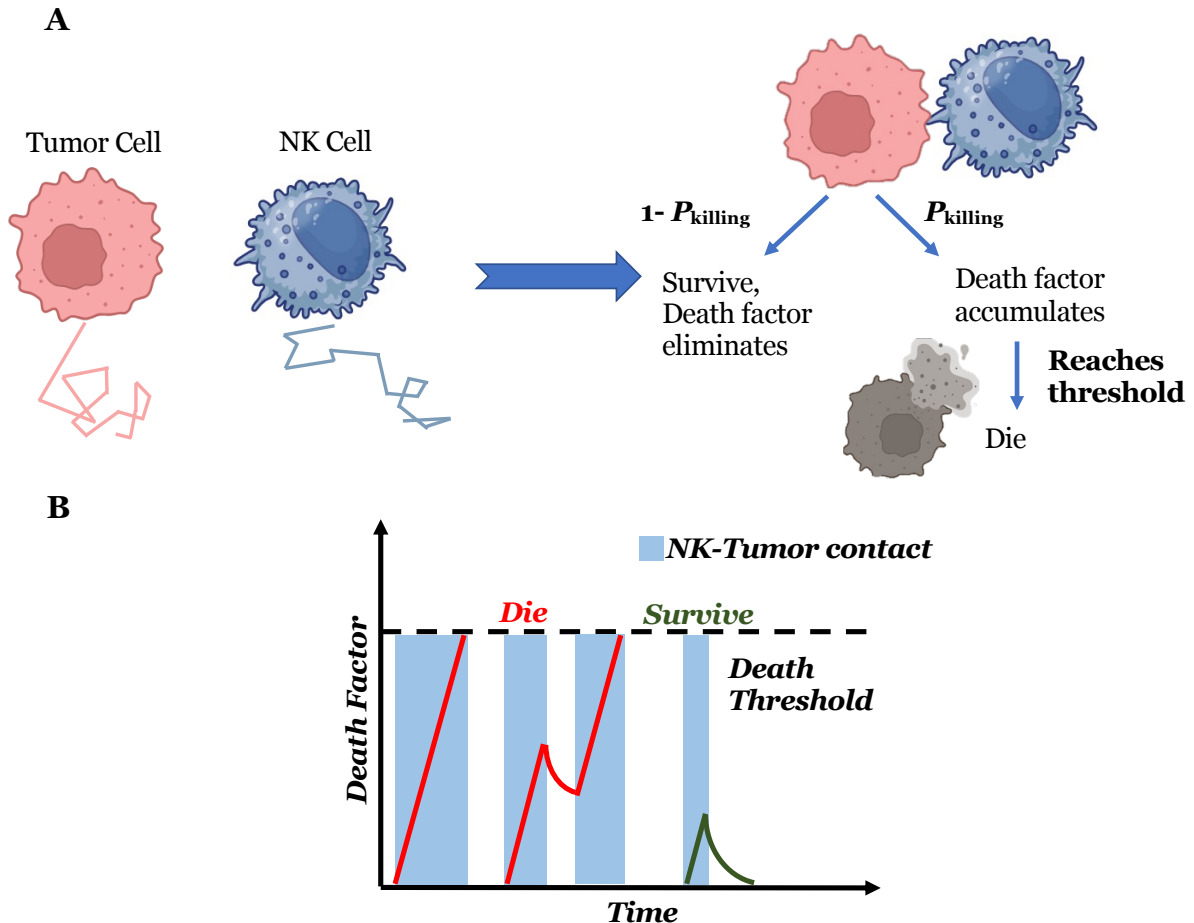


Figure 4. The modelling design of NK-tumour cell interactions. (A) NK cell and tumour cells are described as random walk. Each NK cell is assigned with a killing probability ($P_{killing}$). When NK and tumour cell have contact, the killing decision is made based on the $P_{killing}$ and the molecular pattern at contact site. If decision is to kill, death factor accumulate. If not, tumour cell survives at this contact and death factor starts to decrease. (B) The dynamic of death factor during and after the NK-tumour contact, resulting in distinct killing outcomes.

2.1.3 Tumour Death Factor Dynamics

If killing decision to kill is made, the tumour death factor, reflecting damage and recovery of tumour cell balance, starts to accumulate. Once death factor surpasses a certain threshold, the tumour cell is killed and no longer interacts with other NK cells. If contact is interrupted, the accumulation of death factor stops and elimination of death factor starts. The dynamics of death factor is shown on Figure 4B, which is captured by using following ordinary differential equation:

$$\frac{d\chi}{dt} = \kappa - \phi\chi \quad (Eq. 11)$$

where variable χ denotes death factor, parameter κ denotes accumulation rate and parameter ϕ denotes elimination rate. Every tumour j is assigned an initial death factor χ_j from a uniform distribution between 0 and 5. If χ_j exceeds the death threshold constant χ_T , tumour cell will be marked as killed and ignored in following simulation. Variable χ could reach steady state $\frac{\kappa}{\phi}$ if NK-tumour contact is not interrupted. Therefore, death threshold χ_T should be defined as a value below $\frac{\kappa}{\phi}$ as tumour cell death factor can never exceeds steady state value. The tumour cell death factor is eliminated by setting $\kappa = 0$ in the Eq.11 if no NK-tumour cell interaction takes place or NK cell does not initiate cytotoxic response. Eq.11 is implemented numerically through Euler algorithm:

$$\chi(t + dt) = \chi(t) + (\kappa - \phi\chi) \cdot dt \quad (Eq. 12)$$

Constant parameters among simulation are listed in Table 1A. For temporal evolution of tumour killing simulation (section 3.2), total time of 20 hours is used. In section 3.1.2 and 3.3, total cell population 400 was used with a E:T ratio of 1:3. Parameters controlling cell motility are kept constant (Table 1B), except section 3.1.2 where parameters for NK motility were manipulated.

Table 1A. Constant parameters used in the simulations

L	600 μm
r_{NK}	10 μm
r_{Tu}	12 μm
ε	e^{-20}
σ_{TT}	21.38 μm
σ_{NT}	19.60 μm
σ_{NN}	17.82 μm
χ_T	5
χ	0-5
$P_{killing}$	0.55-0.6
κ	4 hour ⁻¹
ϕ	0.2 hour ⁻¹
Δx_{max}	5 μm
T	8 hours
dt	1/20 hours

Notation

L : Domain length	r_{NK} : NK cell radius
r_{Tu} : Tumour cell radius	ε : Epsilon
σ_{TT} : Sigma of tumour-tumour cell interaction	
σ_{Tu} : Sigma of NK-tumour cell interaction	
σ_{NN} : Sigma of NK-NK cell interaction	
χ_T : Death factor threshold	χ : Death factor
$P_{killing}$: NK killing probability	κ : Death factor accumulation rate
ϕ : Death factor elimination rate	Δx_{max} : Maximum displacement of cells
T: Total time	dt: Initial timestep

Table 1B. Parameters controlling cell motility used in simulations

	γ (hour ⁻¹)	\mathbf{g} ($\sqrt{\text{hour}^{-1}}$)	β ($\mu m/\text{hour}$)	\mathbf{b} ($\mu m \cdot \sqrt{\text{hour}^{-1}}$)
NK cell	0.02	0.05	50	5
Tumor Cell	0.08	0.1	60	5

2.2 Statistical analysis

The repeats for simulations were run ranging from 3 to 8 times. The mean displacements were calculated measure how far cells move from the starting point on average over a given time interval when manipulating parameters controlling cell motility. The mean displacement is defined as:

$$\text{Mean Displacement } (t) = \sqrt{\langle [r(t) - r(0)]^2 \rangle} \quad (\text{Eq. 13})$$

Since data was not normally distributed and the repeats were relatively small, non-parametric Mann-Whitney U test, was applied when conducting pairwise comparison between groups. For multiple pairwise comparisons in section 3.3, Bonferroni correction was employed to adjust multiple testing and reduce the likelihood of type I errors. Median and interquartile (IQR) were used to report the central tendency and variability, and were also applied in visualising error bars, which minimises the influence of outliers and skewed distributions compared with means and standard deviations.

All code was implemented in Python 3.13.2 and executed within Visual Studio Code (VS code). NumPy (Harris et al., 2020) and pandas (McKinney, 2010) were utilized to construct and manage numerical arrays and tubular data structures for simulation and analysis. SciPy was used for statistical analysis (Virtanen et al., 2020). Seaborn (Waskom, 2021) and matplotlib (Hunter, 2007) were used for visualization.

Chapter 3 Results

The snapshots of an 8-hour simulation of NK-tumour cell interactions between 100 NK cells and 200 tumour cells is shown on Figure 5, which provide information about cell distributions, cell trajectories and killing outcomes at the start (hour 0) and end of the simulation (hour 8) based model.

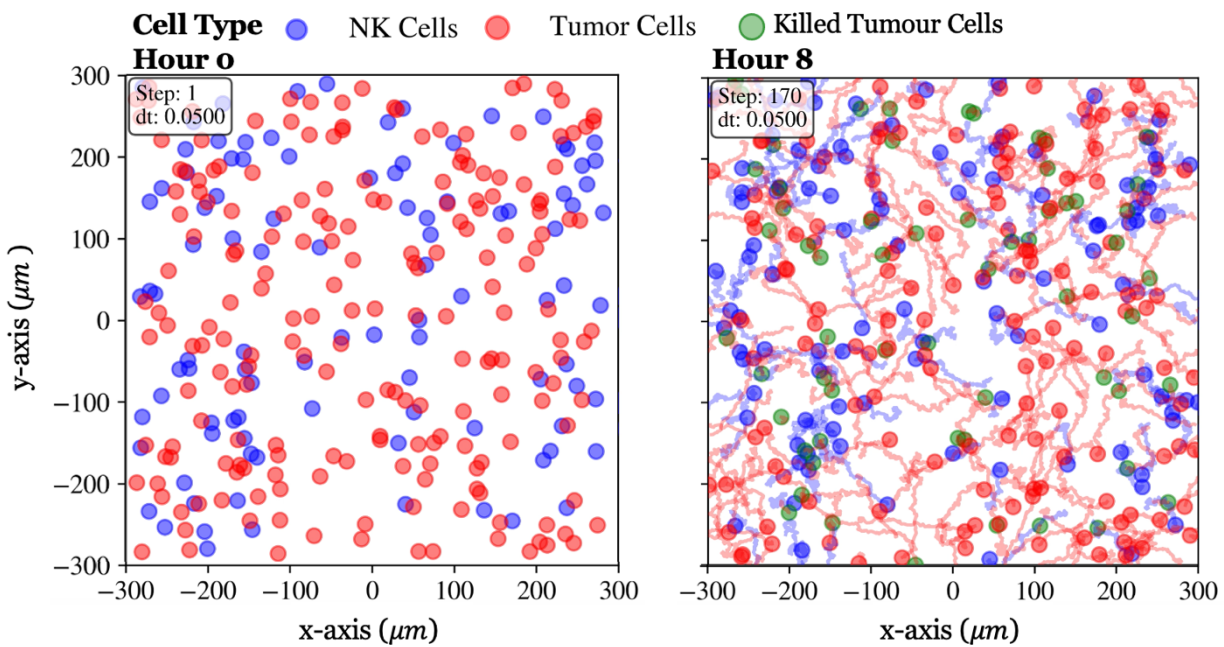
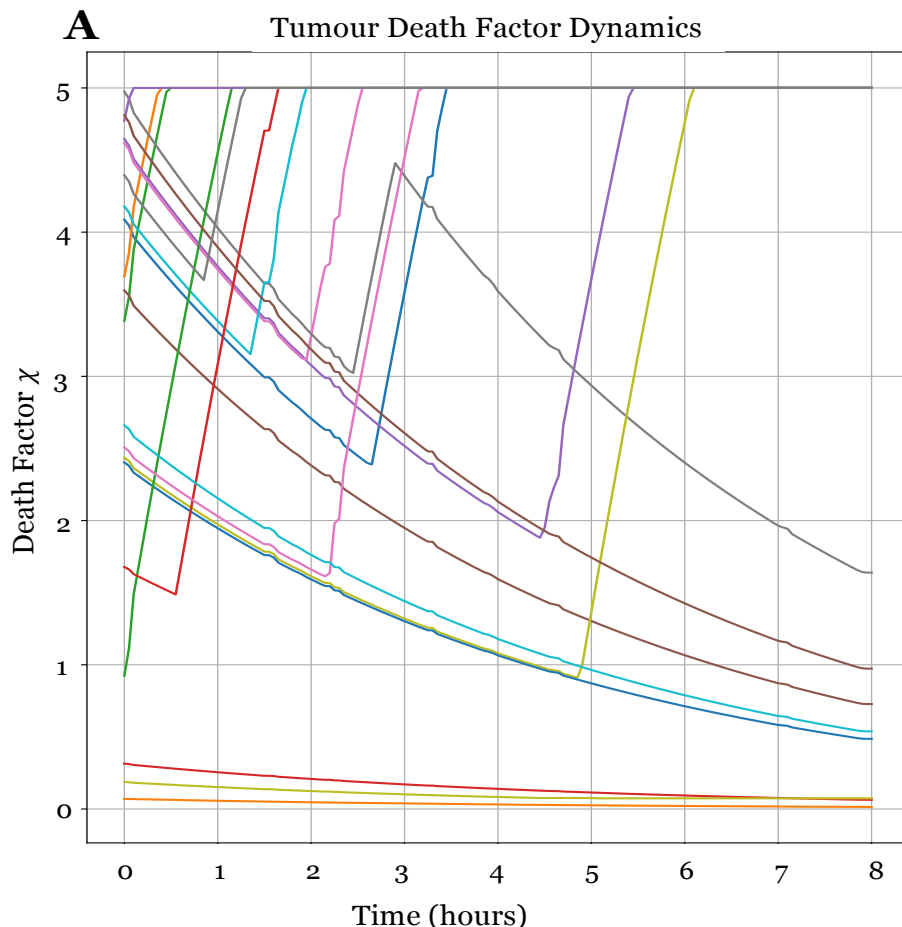


Figure 5. The snapshots of simulation of NK cell mediated cytotoxicity at hour 0 and hour 8. 100 NK cells and 200 tumour cells are involved in this simulation. Blue particles indicate the NK cells, red particles indicate tumour cells and green particles refer to the dead tumour cells.

To demonstrate model's ability to simulate the NK cell mediated cytotoxicity, an 8-hour simulation involving 50 NK cells and 250 tumour cells with a death threshold χ_T of 5 was performed. Based on Eq.11, the minimum time of contacts to reach χ_T is varied depending on their initial death factors. Figure 6A displays temporal evolution of death factor of 20 tumour cells. Tumour cells exhibit various death tumor dynamics depending on their interactions with NK cells. Target cells without contacts or where killing was not initiated

show continuous decay of death factor until reaches zero. Tumour cells contact with activated NK cells exhibit death factor accumulation during contact. Tumours with lower initial death factors require longer contact duration to reach death threshold. The elimination of death factor resumes when contact with NK cell exhibiting cytotoxicity was interrupted. These patterns matched the idea of contact-related death factor dynamics that proposed in section 2.1.2.

Figure 6B illustrates number of contacts and killing outcome for each contact, called contact history in 8 hours. 8% of NK cells showed no interaction, 16% of NK cells were exhausted, 24% of NK cells showed non-killing behaviour, 24% of cells exhibited killing behaviour and 44% of NK cells were observed stochastic switching between non-killing and killing outcomes at different contacts. Therefore, model effectively captured the stochastic nature of NK cell mediated cytotoxicity.



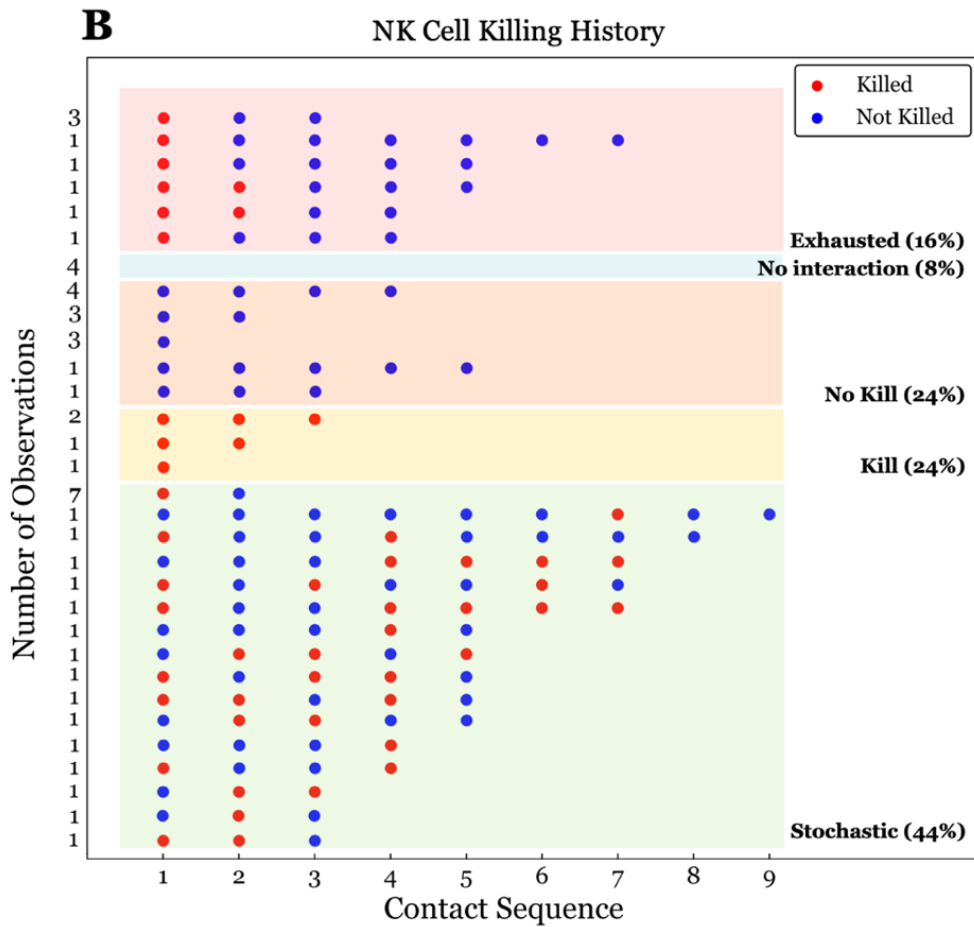


Figure 6. An 8-hour simulation of NK-tumour cell interactions involving 50 NK cells and 250 tumour cells. (A) The temporal evolution of death factor dynamics of 20 tumour cells. Each line represents a tumour cell. (B) The contact history of NK cells. Each row represents a sequence of contacts and killing outcomes of NK cell. Number of observations indicates the number of NK cells exhibited identical contact history. Five distinct classes of NK killing behaviours are highlighted in different colours with the proportion of NK cells in each class relative to the total NK population.

Following this, different parameters were explored to understand their impacts on NK killing outcomes. The parameters controlling cell motility were altered to understand their effects on cell motility and NK cell killing outcomes. Moreover, effector-to-target ratios (E:T), a critical parameter for immune-tumour interactions that influencing likelihood of NK cell engagement and tumour cell elimination, were manipulated to assess its impacts on population-level outcomes. Death factor thresholds, as tumour cell sensitivity, were altered to look at how different death factor thresholds affect killing outcomes.

3.1 Manipulating Cell Motility Parameters

3.1.1 Impacts of cell motility in cell trajectories

Based on Eq.2 and Eq.7, γ and g affect the cell polarity while β and b impact cell position.

These parameters were manipulated and explored to understand how they influence cell motion.

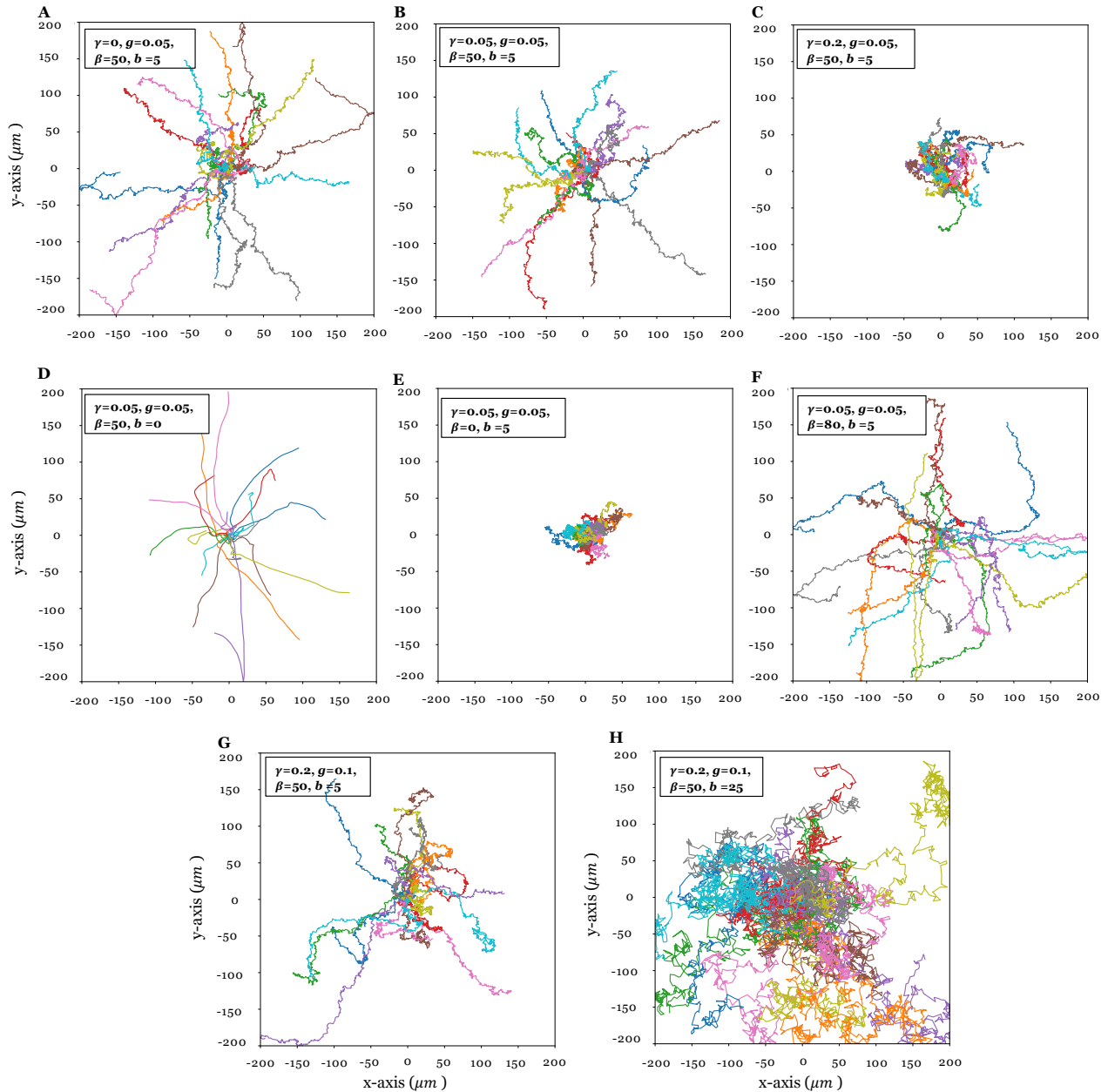


Figure 7. Cell trajectories under different γ , g , β and b combinations. Each plot shows 20 independent cell trajectories, all starting at the origin (0,0).

Four parameters (γ , g , β and b) influence cell motion in distinct ways. γ controls the rate at which cell polarisation decays to zero. Comparing Figure 7A, 7B & 7C, higher γ value leads to more localised motility (less persistent) since it cannot maintain its current direction over time. β regulates relationship intensity between cell polarity and velocity. Higher β value results in larger cell displacement, see Figure 7E -F. The mean displacements at fifth hours between two groups ($\beta = 0$ and $\beta = 80$) were compared, see Figure 8. Group with $\beta = 80$ (median = $60.65 \mu m$) had a significantly larger displacement comparing with group with $\beta = 0$ having median of $15.84 \mu m$ ($U = 0$, p -value = 0.008). Simulation with $\beta = 0$ showed situation where cell motility is independent to polarity and only rely on the noise of cell velocity, b . Higher b value results in a noisy and jagged cell trajectory (Figure 7G-H). When $b = 0$, cell position changes are noise-free, resulting in a persistent and linear motion until hitting the boundary, see Figure 7D. Based on Figure 7C and 7G, higher value of parameter g controlling intensity of cell polarity shows more expansive trajectory.

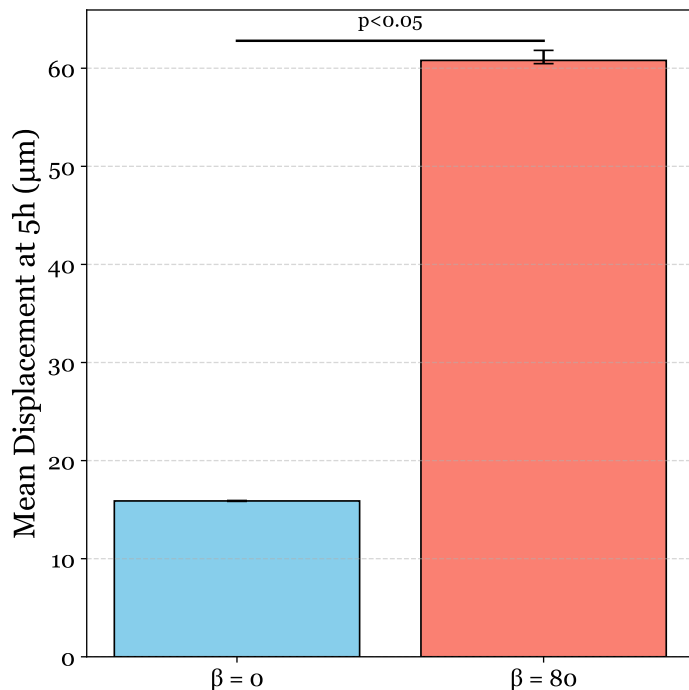


Figure 8. Displacement comparison between $\beta = 0$ and $\beta = 80$. Error bars indicate the interquartile (IQR). Statistical significance is determined by using Mann-Whitney U test.

3.1.2 Impacts of cell motility on NK killing outcomes

From section 3.1.1, parameter γ , g , β and b influence cell motion in its distinct way respectively, which potentially could affect interaction details between cells, e.g., frequency of having contact and contact duration. In this section, these parameters were explored to investigate their impacts on NK-tumour interactions and NK cell killing profiles.

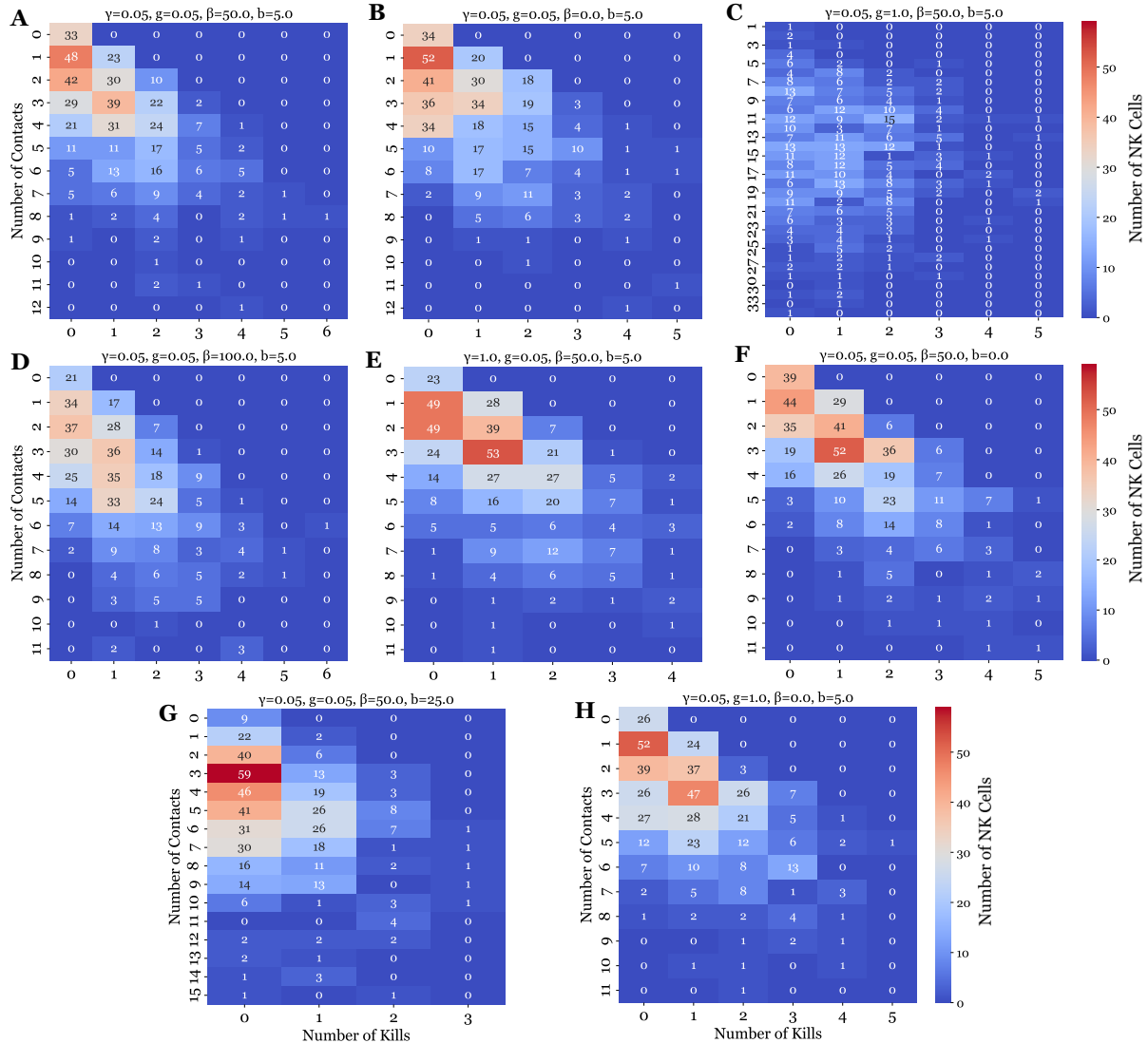


Figure 9. The heatmaps of NK cell contacts and kills combined across five replicates per parameter set. x-axis is number of kills and y-axis is the number of contacts of NK cells. The colour bar indicates the number of NK cells having a specific number of contacts and kills.

Figure 9 shows heatmaps of NK cell contacts and kills combined across five replicates per parameter set. Compare panels A and E, both exhibit a similar diagonal trend between

number of contacts and number of killings with high NK cell frequencies clustered in the upper left, indicating many cells made few contacts and kills. Despite altering γ , the median of total kills and total contacts remains comparable: 102 (IQR: 102-107) for $\gamma = 0.05$ and 104 (IQR: 101-104) for $\gamma = 1$. However, lower γ value permits greater per-cell killing capacity (up to 6), while higher gamma limits kill to a maximum of 4. This may relate with difference in contact durations that median of contact duration was 62.07 minutes at $\gamma = 0.05$ and 57.66 minutes at $\gamma = 1$. Noticeably, there is no significant difference between fraction of tumour killed comparing high persistent movement ($\gamma = 0.02$) and low persistent movement ($\gamma = 0.2$) ($U = 19.5$, p -value = 0.807). However, the fraction of tumour killed for $\gamma = 0.02$ shows smaller variability comparing with group with $\gamma = 0.2$ even though their medians are similar where 0.38 for $\gamma = 0.02$ and 0.377 for $\gamma = 0.2$ (Figure 10).

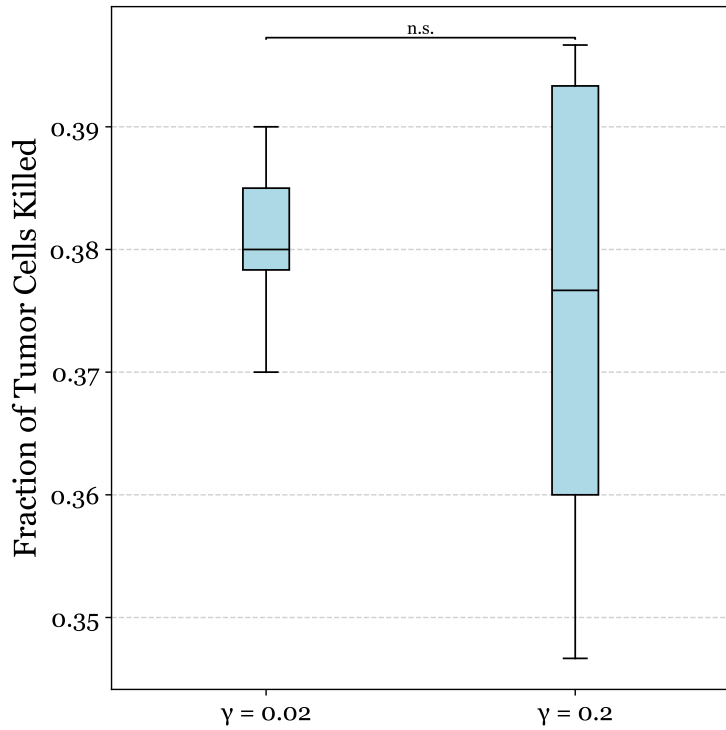


Figure 10. Fraction of tumour cell killed comparison between group $\gamma = 0.02$ and $\gamma = 0.2$. The error bars indicate the median and IQR. Statistical significance is determined using Mann–Whitney U test. n.s. denotes no significant difference in killing fraction between two groups.

For Figure 9F where $b = 0$, NK cell typically made a small number of contacts (0–6) and a small subset of these resulted in successful killing. A diagonal trend is visible, indicating a positive relationship between number of contacts and number of kills. In Figure 9G, increasing noise intensity for cell ($b = 25$) results in a broader distribution of contacts (0–9) with some NK cells making over 10 contacts. Few NK cells have zero contact with tumour cells. However, the number of kills per cell remains low with a maximum killing capacity of 3 for $b = 25$ and of 5 when $b = 0$. The median contact duration at $b = 25$ was 11.94 minutes (IQR: 3.74–24.02 minutes) and 87.02 minutes at $b = 0$ (IQR: 30.00–157.83 minutes). The killing frequency, defined as number of kills divided by number of contacts, drops from 37.1% (IQR: 36.8%–37.3%) at $b = 0$ to 8.61% (IQR: 8.37%–8.97%) at $b = 25$. This may suggest that high noise intensity impairs NK cell killing efficiency due to shorter contact.

Comparing Figure 9A and C, parameter g strongly influences contact frequency. A larger g value ($g = 1$) results in median of 14 contacts per NK cell (IQR: 10–19), compared to 3 (IQR: 2–5) when $g = 0.05$. This increase in contact frequency shortens median of contact duration from 62.04 minutes ($g=0.05$) to 15.18 minutes at $g = 1$. However, parameter g has little impact on total kills and capacity of per NK cell killing where total kills were 108 (IQR: 106–110) for $g = 1$ and 102 (IQR: 102–107) for $g = 0.05$.

Comparing Figure 9B and D, increased β value leads to greater number of NK cells having frequent contacts with tumour cells. When $\beta = 100$, 66.0% of NK cells achieved at least one kill, compared to 56.6% at beta=0. Importantly, more NK cells engaged in frequent contacts (≥ 8 contacts) at $\beta = 100$ (count: 19 vs. 6) and performed multiple killings (≥ 2 kills) at $\beta = 100$ (14 vs. 5). Therefore, median of total killing outcomes was 106 (IQR: 106–119) total killing when $\beta = 100$ while a median of 97 (IQR: 79–97) when $\beta = 0$. A notable finding was observed that increasing β value does not affect number of contacts when g staying at 0.05 (Figure 8B&D). In contrast, when $g=1.0$, increased β value from 0 to 50

leads to a substantial increase in the number of contacts, see Figure 9C and 9H. These observations may indicate an interaction effect between β and g that effect of g on number of contacts is dependent on the level of β .

3.2 Impacts of E:T ratio on NK killing outcomes

Next, we investigate how ratio of NK to tumour cells influence cytotoxic dynamics by changing initial density and proportions of each cell type.

Table 2. Initial E:T Ratios and their corresponding number of cells at different total cell population

E:T Ratio	Total = 100	Total = 500	Total = 1000
1:20	5 : 95	24 : 476	48 : 952
1:10	9 : 91	45 : 455	91 : 909
1:5	17 : 83	83 : 417	167 : 833
1:2	33 : 67	167 : 333	333 : 667
1:1	50 : 50	250 : 250	500 : 500
2:1	67 : 33	333 : 167	667 : 333
5:1	83 : 17	417 : 83	833 : 167
10:1	91 : 9	455 : 45	909 : 91
20:1	95 : 5	476 : 24	952 : 48
99:1	99 : 1	495 : 5	990 : 10

The simulations were run at different E:T ratio and different total cell populations, see Table 2. By using a fixed domain length of $600 \mu m$, different total cell populations result in varied cell densities with different levels of crowding, see Figure 11. Boundary cases with a single NK or tumour cell at varying total populations were also simulated.

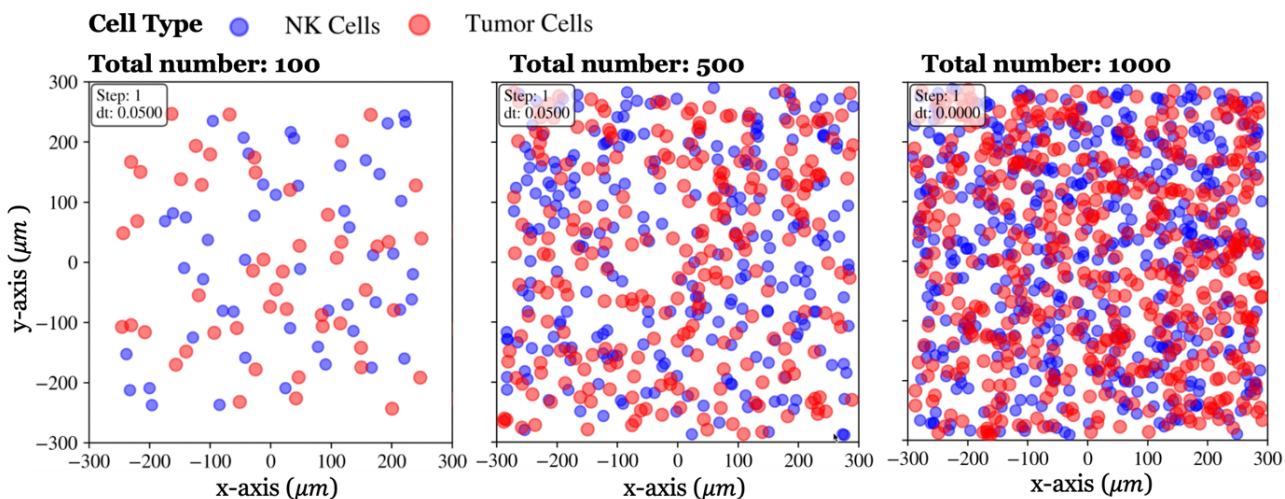


Figure 11. Cell distribution within a defined domain at total number of 100, 500 and 1000 at a constant E:T ratio of 1:1. Smaller total number results in lower cell density and therefore lower level of crowding. Blue particles indicate the NK cells and red particles indicate tumour cells.

Comparing with low cell density (blue line), high cell density (green line) has a consistently high percentage of tumour cell killed across all E:T ratios (Figure 12). For instance, at E:T of 2:1, 33.3% (IQR: 27.3% – 36.4%) of tumour cells were killed when total population was 100. In contrast, 80.5% tumour cell killing was observed when total population was 1000. For all cell densities, increase of E:T ratio value leads to larger fraction of tumour cells being killed. From E:T = 1:20 to 2:1, each group showed large increased fraction of tumour killed comparing with its lower E:T value, followed by a more gradual slope of increase beyond E:T = 2:1.

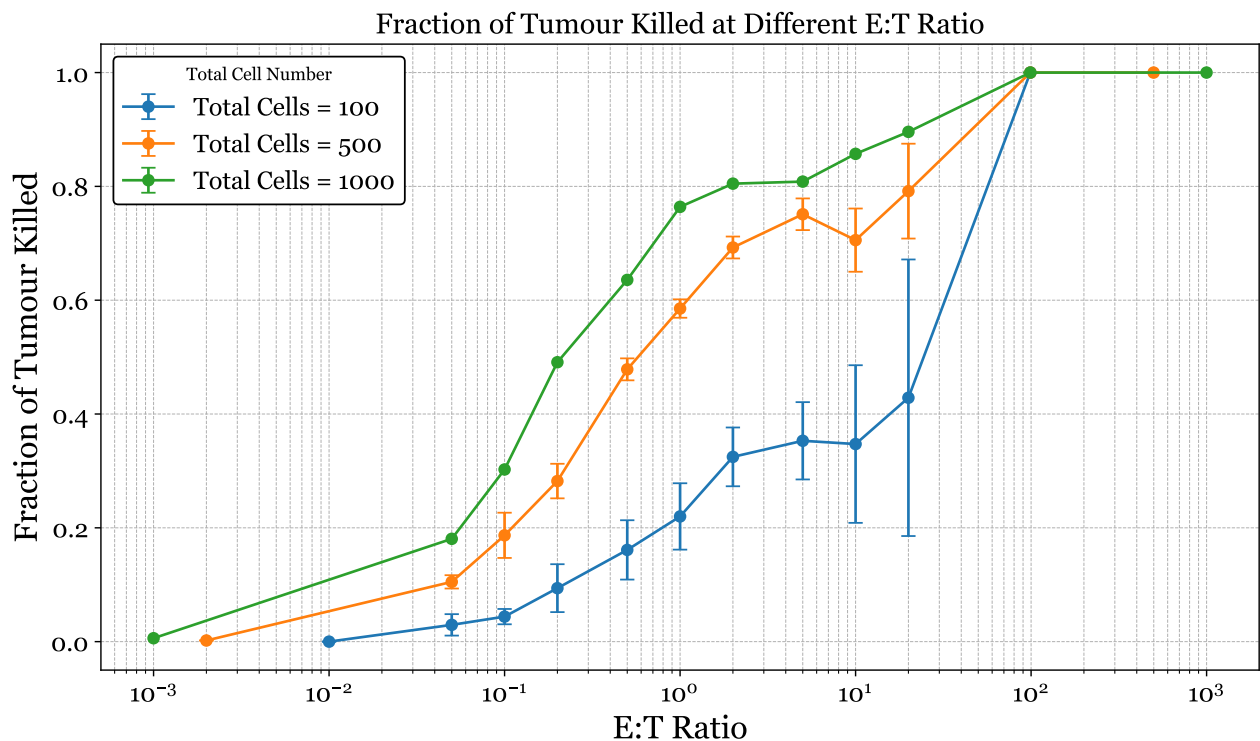


Figure 12. Fraction of tumour cells killed by NK cells at different E:T ratios for 8 hours simulation. Each line represents a total cell population. By running simulation under a fixed domain area, the cell density varies. E:T ratios are plotted in a log scale to capture the wide range of values. Each point indicates the median and with the error bar representing the interquartile range (IQR).

The temporal evolution of tumour killing across E:T ratio was also explored to understand how NK cells cytotoxicity progresses over time. The patterns in Figure 13A were consistent with pattern shown in Figure 12 that higher E:T ratio leads to larger proportion of tumour cells being killed. Most tumour killing events finish before 10 hours. For E:T ratio below 1:1, slope of tumour killing curve remains shallow before 10 hours. As the E:T ratio beyond 1:1, slope become noticeably steeper, indicating better rate of tumour killing. From Figure 13B, at E:T = 1:20 to 1:5, increase of tumour killed proportion is identical before and after 5 hours. However, the largest increase of fraction of tumour killing happened before 5 hours for E:T ratios ranging from 1:2 to 20:1. Between 15 and 20 hours, the fraction of tumour killed increased in an extremely slow rate. Besides, fraction of tumour killed reaches a plateau beyond E:T=5:1 in long period, i.e., 20 hours. Median fraction of tumour killed for

$E:T = 5:1$ was 84.3% (IQR = 81.3% – 86.7%), for $E:T = 10:1$ was 80.0% (IQR = 78.9% – 83.3%), for $E:T = 20:1$ was 83.3% (IQR = 81.3% – 85.4%), which is consistent with observation in Figure 12 showing slower increase of tumour killing between high $E:T$ ratio.

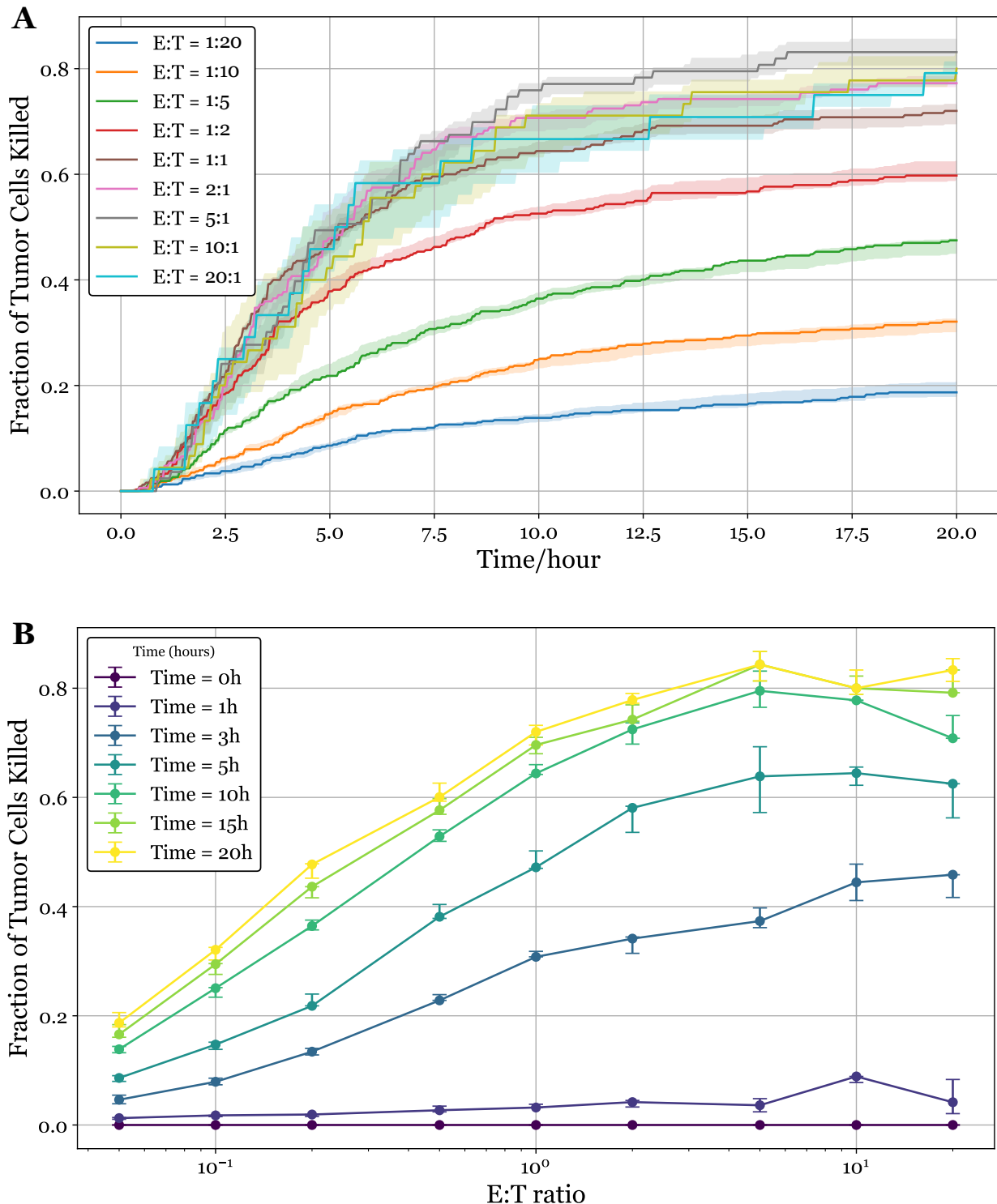


Figure 13. The temporal evolution of fraction of tumour killing (A) over 20 hours. Each line represents median of fraction of tumour killed at a specific E:T ratio. The shading areas indicate the IQR. (B) across different E:T ratio. Each line represents the

median of fraction of tumour killed at a time frame (ranging from 0 hour to 20 hour). The error bars indicate the IQR. E:T ratios are plotted in a log scale.

3.3 Effects of death factor threshold on NK killing outcomes

In this section, we explored how death factor threshold could influence NK killing outcomes. From Figure 14, increase of death factor threshold leads to significant decrease of tumour cells being killed. At a death threshold of 2, the median fraction of tumour killed was 46.7% (IQR: 44.0%–47.0%), compared to 4.67% (IQR: 4.0%–4.67%) when death factor threshold was set to 16, a tenfold reduction in killing ($p < 0.05$). These data clearly show a correlation between death factor thresholds and proportion of tumour killed.

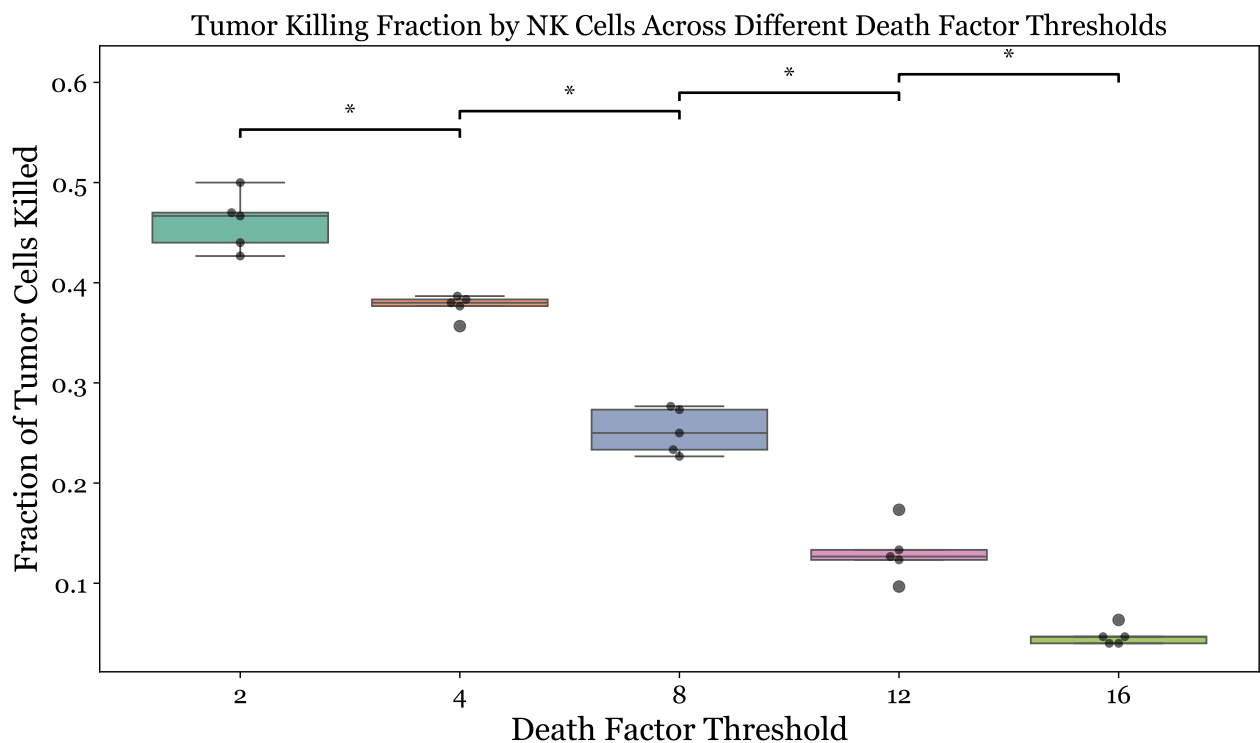


Figure 14. The fraction of tumour cell killed across different death factor thresholds ranging from 2 to 16. Error bars indicate the interquartile (IQR). Statistical significance is determined using Mann–Whitney U test. Asterisks (*) denote statistically significant differences in killing fraction between each threshold and the previous one on sequence with $p < 0.05$.

Chapter 4 Discussion

This model provides individual-level resolution such as death factor dynamic for individual tumour cells and detailed contact histories, referring the property of ABM. Moreover, model successfully observed five distinct classes of NK killing behaviours reported in Vanherberghen et al., therefore effectively captured stochastic nature of NK cell mediated cytotoxicity. Based on this, it may suggest no cellular intrinsic heterogeneity between stochastic NK killers and serial killers; the observed difference arise from stochastic dynamics as NK cells are assigned similar initial $P_{killing}$ in the model. Time-lapse microscopy of NK cell-tumour interactions observed expression of CD8 α is related to high levels of serial killing (Rey et al., 2025). However, expression profile of stochastic NK killer remains unclear. To check the presence of cellular intrinsic differences between these two classes of NK cells experimentally, microwell-based platform could be used to identify and sort them (Guldevall et al., 2016). Single-cell RNA sequencing (scRNA-seq) and cellular indexing of transcriptomes and epitopes by sequencing (CITE-seq) then could be applied and help in identification of cell surface protein and transcriptomic heterogeneity between two groups of NK cells, which has been conducted and identified three prominent NK cell subsets in human blood (Rebuffet et al., 2024).

For parameter explorations, parameter γ , g , β and b were found to affect NK-tumour interaction in distinct ways. Results suggest that γ may controls per-cell killing capacity, while b affects both the number of contacts (i.e., searching ability) and its killing capacity. These effects align with observed changes in cell motility patterns when varying γ and b (see Section 3.1). A lower γ leads to slower restoration of cell polarity resulting in prolonged direction persistence and therefore enabling longer interaction time, which

enhances the killing capacity. The finding is consistent with the study that observed the presence of bystander cells enhances the NK killing efficiency by increasing its persistence (Zhou et al., 2017). A higher noise intensity in cell displacement b produces a more erratic trajectory that increase frequency of contacts but often lead to shorter contact durations since cell positions change drastically. Therefore, number of kills per NK cell is low. Notably, an interaction effect was observed between g and β . High g value only results in increased contact number when $\beta \neq 0$, indicating cell motility must be governed by polarity to increase contact number through increasing g . Future studies could systematically explore how varying β modulates effect of g on contact frequency. In addition, other interaction effects may remain unidentified as changes on heatmaps are subtle and therefore hard to identify. Statistical analysis could help to uncover these hidden interaction effects. Overall, model offers a mechanistic understanding on how directional persistence and displacement affect contact dynamics and killing outcomes, which highlights importance of cell motility in shaping NK-tumour cell interaction and NK cytotoxic response. This is consistent with previous *in vitro* experimental observations that migration behaviours of CTLs, which share similar cytotoxic mechanisms with NK cells, significantly influence on immune response effectiveness (Sadjadi et al., 2020).

Higher total cell density enhances NK cell killing outcomes. This enhancement likely results from increased opportunities for NK-tumour contacts at high density, which facilitates multiple and frequent contacts with tumour cells. Based on death factor dynamics, death factor would accumulate during contacts, therefore, frequent contacts could lead to better killing outcomes. Such explanation is consistent with concept called additive cytotoxicity previously reported in CTLs where multiple sublethal hits could accumulate to induce tumour death (Weigelin et al., 2021). However, the rate of improvement in killing efficiency appears to diminish at higher densities. The increase in fraction of tumour killed between total population 500 and total population 1000 is

notably smaller than increase from total population 100 to 500. While large error bars were shown when cell density is small, requiring more repeats for more robust results, this trend may still suggest the impact of cell density could be saturated at a certain cell density. Interestingly, a study found that reducing cell density observed a significant improvement in percent specific lysis of K562 cell (Somanchi et al., 2015). This may be explained due to overcrowded environment causing jamming behaviour that cell movement is significantly reduced as observed in epithelial cells at high cell density (Nnetu et al., 2013). While this phenomenon has not been directly demonstrated in NK-tumour interactions, it is plausible that similar biophysical constraints could arise at high cell densities and may have negative impacts on tumour killing when surpassing certain cell density. To test whether jamming happens in our simulation and identify critical density at which negative impacts on tumour killing occurs, future simulation need include larger cell populations (e.g., 2000 or more cells). However, it would be extremely computationally expensive and time-consuming, therefore leveraging high-performance computing is essential for efficient simulation.

The observation that higher E:T ratio results in increased fraction of tumour cells being killed from simulation aligns with prior *in vitro* findings. For example, IFN- γ secretion, directly proportional with NK cell tumoricidal activity, increased as E:T ratio rose from 1:2 to 2:1 in NK-A549 cell interaction (Gong et al., 2015). Same trend was also observed in the percentage of lysis of K562 cell in interaction with NK cells using image cytometry (Somanchi et al., 2015). Together, results highlight the importance of NK cell availability in optimising NK cell-mediated tumour cell killing. However, simulation results also suggest that this effect may not be scale infinitely. The fraction of tumour killed would reach a plateau in a long period of time, e.g., 20 hours where 5:1 ratio does not show significant difference in fraction of tumour killing with 20:1 ratio. E:T ratio of 5:1 is suggested to be

sufficient for effective NK killing under a certain condition. Extremely high E:T ratio is not necessary to be tested experimentally, which increases costs in the practical.

Death factor threshold could refer tumour vulnerability to NK cytotoxicity. An inverse linear relationship between death factor threshold and fraction of tumour cell killed was observed. This is consistent with observation that highly sensitive tumour, for example expressing high level of greater surface expression of NKG2D ligands and death receptors Fas and DR5, are more susceptible to killing (Ames *et al.*, 2015). Simulation results support the idea that therapeutical strategies that sensitise tumour cells – such as low dose ionizing radiation, which could upregulate expression of activating ligands and decrease the expression of HLA class I molecules - enhancing NK cell effectiveness (Yang *et al.*, 2014) . Combining tumour sensitizing strategy appropriately, efficiency of NK cell-based therapy could be enhanced. Moreover, varying γ is altered while keeping death factor threshold constant can yield similar NK killing outcomes but with different variability level, see Figure 10. Reducing this variability would also be beneficial for effective treatment. By exploring more combinations of parameters in the future, this could be understood and facilitates efficiency of NK cell-based therapy.

Overall, this ABM highlights the importance of cell motility in shaping NK-tumour cell interaction and cytotoxic response, suggesting an optimal E:T ratio for experiments and provides insights in enhancing efficiency of NK cell-based therapy. Following future parameter fitting using experimental data through Bayesian inference-guided estimation, this model could be applied to test hypotheses regarding stochastic NK-cell mediated cytotoxicity. By comparing killing outcomes with and without inclusion of probabilistic killing decision from simulations, this helps to verify our hypothesis on stochastic killing behaviour. Additionally, predictivity of model will be tested by assessing how well simulation results match with experimental result. Current model incorporates constant NK killing probability for each NK cell and a constant decreasing value after each contact

representing NK cell exhaustion. By implementing temporal dynamic of activating and inhibitory receptors and ligands expression related with contact number, simulation is more realistic and comprehensive for mirroring NK cell- mediated cytotoxicity. After refinement of model and validation of model predictivity, NK killing outcomes could be predicated when interacting with varied tumour cells whose parameters are determined by parameter fitting. Through parameter scan for NK cell, parameters that resulting in optimal killing behaviours for a specific type of tumour could be determined, which acts as a powerful tool and provides valuable insights on designing and enhancing NK cell-based immunotherapy.

Reference

- Ames, E. et al. (2015) *NK Cells Preferentially Target Tumor Cells with a Cancer Stem Cell Phenotype*. *The Journal of Immunology*, 195(8), pp. 4010–4019. DOI: <https://doi.org/10.4049/jimmunol.1500447>.
- Bonabeau, E. (2002) *Agent-based modeling: Methods and techniques for simulating human systems*. *Proceedings of the National Academy of Sciences*, 99(suppl_3), pp. 7280–7287. DOI: <https://doi.org/10.1073/pnas.082080899>.
- Cess, C.G. and Finley, S.D. (2020) *Multi-scale modeling of macrophage–T cell interactions within the tumor microenvironment*. *PLoS Computational Biology*, 16(12), p. e1008519. DOI: <https://doi.org/10.1371/journal.pcbi.1008519>.
- Elephes Sung (2024) *Theoretical Modelling of the Stochastic Natural Killer Cell-Mediated Cytotoxicity*. *Unpublished Master's Thesis, Imperial College London*.
- Gong, C. et al. (2015) *A High-Throughput Assay for Screening of Natural Products that Enhanced Tumoricidal Activity of NK Cells*. *Biological Procedures Online*, 17(1), p. 12. DOI: <https://doi.org/10.1186/s12575-015-0026-6>.
- Gong, C. et al. (2017) *A computational multiscale agent-based model for simulating spatio-temporal tumour immune response to PD1 and PDL1 inhibition*. *Journal of The Royal Society Interface* [Preprint]. DOI: <https://doi.org/10.1098/rsif.2017.0320>.
- Goyco Vera, D. et al. (2024) *Approved CAR-T therapies have reproducible efficacy and safety in clinical practice*. *Human Vaccines & Immunotherapeutics*, 20(1), p. 2378543. DOI: <https://doi.org/10.1080/21645515.2024.2378543>.

Guldevall, K. *et al.* (2016) *Microchip Screening Platform for Single Cell Assessment of NK Cell Cytotoxicity*. *Frontiers in Immunology*, 7, p. 119. DOI: <https://doi.org/10.3389/fimmu.2016.00119>.

Handel, A., La Gruta, N.L. and Thomas, P.G. (2020) *Simulation modelling for immunologists*. *Nature Reviews Immunology*, 20(3), pp. 186–195. DOI: <https://doi.org/10.1038/s41577-019-0235-3>.

Harris, C.R. *et al.* (2020) *Array programming with NumPy*. *Nature*, 585(7825), pp. 357–362. DOI: <https://doi.org/10.1038/s41586-020-2649-2>.

Horowitz, A. *et al.* (2013) *Genetic and environmental determinants of human NK cell diversity revealed by mass cytometry*. *Science translational medicine*, 5(208), p. 208ra145. DOI: <https://doi.org/10.1126/scitranslmed.3006702>.

Hu, Y.S., Cang, H. and Lillemeier, B.F. (2016) *Superresolution imaging reveals nanometer- and micrometer-scale spatial distributions of T-cell receptors in lymph nodes*. *Proceedings of the National Academy of Sciences of the United States of America*, 113(26), pp. 7201–7206. DOI: <https://doi.org/10.1073/pnas.1512331113>.

Hunter, J.D. (2007) *Matplotlib: A 2D Graphics Environment*. *Computing in Science & Engineering*, 9(3), pp. 90–95. DOI: <https://doi.org/10.1109/MCSE.2007.55>.

Jones, J.E. and Chapman, S. (1924) *On the determination of molecular fields.—I. From the variation of the viscosity of a gas with temperature*. *Proceedings of the Royal Society of London. Series A, Containing Papers of a Mathematical and Physical Character*, 106(738), pp. 441–462. DOI: <https://doi.org/10.1098/rspa.1924.0081>.

Konjević, G. *et al.* (2009) *Distribution of Several Activating and Inhibitory Receptors on CD3–CD16+ NK Cells and Their Correlation with NK Cell Function in Healthy*

Individuals. Journal of Membrane Biology, 230(3), pp. 113–123. DOI:

<https://doi.org/10.1007/s00232-009-9191-3>.

Lingwood, D. and Simons, K. (2010) *Lipid Rafts As a Membrane-Organizing Principle*.

Science, 327(5961), pp. 46–50. DOI: <https://doi.org/10.1126/science.1174621>.

Liu, E. et al. (2020) *Use of CAR-Transduced Natural Killer Cells in CD19-Positive*

Lymphoid Tumors. New England Journal of Medicine, 382(6), pp. 545–553. DOI:

<https://doi.org/10.1056/NEJMoa1910607>.

Mailankody, S. et al. (2023) *Allogeneic BCMA-targeting CAR T cells in*

relapsed/refractory multiple myeloma: phase 1 UNIVERSAL trial interim results. Nature Medicine, 29(2), pp. 422–429. DOI: <https://doi.org/10.1038/s41591-022-02182-7>.

Mallet, D.G. and De Pillis, L.G. (2006) *A cellular automata model of tumor-immune*

system interactions. Journal of Theoretical Biology, 239(3), pp. 334–350. DOI:

<https://doi.org/10.1016/j.jtbi.2005.08.002>.

Martinez, E. et al. (2011) *NKG2D-dependent cytotoxicity is controlled by ligand*

distribution in the target cell membrane. Journal of immunology (Baltimore, Md. : 1950), 186(10), p. 10.4049/jimmunol.1002254. DOI:

<https://doi.org/10.4049/jimmunol.1002254>.

McKinney, W. (2010) *Data Structures for Statistical Computing in Python. in Python in*

Science Conference, Austin, Texas, pp. 56–61. DOI: <https://doi.org/10.25080/Majora-92bf1922-00a>.

Nnetu, K.D. et al. (2013) *Slow and anomalous dynamics of an MCF-10A epithelial cell*

monolayer. Soft Matter, 9(39), pp. 9335–9341. DOI:

<https://doi.org/10.1039/C3SM50806D>.

Pende, D. *et al.* (2019) *Killer Ig-Like Receptors (KIRs): Their Role in NK Cell Modulation and Developments Leading to Their Clinical Exploitation*. *Frontiers in Immunology*, 10. DOI: <https://doi.org/10.3389/fimmu.2019.01179>.

Raulet, D.H. (2003) *Roles of the NKG2D immunoreceptor and its ligands*. *Nature Reviews Immunology*, 3(10), pp. 781–790. DOI: <https://doi.org/10.1038/nri1199>.

Borgert, R. (2021) *Improving outcomes and mitigating costs associated with CAR T-cell therapy*. *The American Journal of Managed Care*, 27(13 Suppl), pp. S253–S261. Available at: <https://doi.org/10.37765/ajmc.2021.88737>.

Rebuffet, L. *et al.* (2024) *High-dimensional single-cell analysis of human natural killer cell heterogeneity*. *Nature Immunology*, 25(8), pp. 1474–1488. DOI: <https://doi.org/10.1038/s41590-024-01883-0>.

Rey, C. *et al.* (2025) *CD8a and CD70 mark human natural killer cell populations which differ in cytotoxicity*. *Frontiers in Immunology*, 16. DOI: <https://doi.org/10.3389/fimmu.2025.1526379>.

Ritter, A.T. *et al.* (2022) *ESCRT-mediated membrane repair protects tumor-derived cells against T cell attack*. *Science*, 376(6591), pp. 377–382. DOI: <https://doi.org/10.1126/science.abl3855>.

Sadjadi, Z. *et al.* (2020) *Migration of Cytotoxic T Lymphocytes in 3D Collagen Matrices*. *Biophysical Journal*, 119(11), pp. 2141–2152. DOI: <https://doi.org/10.1016/j.bpj.2020.10.020>.

Somanchi, S.S. *et al.* (2015) *A Novel Method for Assessment of Natural Killer Cell Cytotoxicity Using Image Cytometry*. *PLoS ONE*, 10(10), p. e0141074. DOI: <https://doi.org/10.1371/journal.pone.0141074>.

Srpan, K. *et al.* (2018) *Shedding of CD16 disassembles the NK cell immune synapse and boosts serial engagement of target cells*. *Journal of Cell Biology*, 217(9), pp. 3267–3283. DOI: <https://doi.org/10.1083/jcb.201712085>.

Subedi, N. *et al.* (2021) *An automated real-time microfluidic platform to probe single NK cell heterogeneity and cytotoxicity on-chip*. *Scientific Reports*, 11(1), p. 17084. DOI: <https://doi.org/10.1038/s41598-021-96609-9>.

Uhlenbeck, G.E. and Ornstein, L.S. (1930) *On the Theory of the Brownian Motion*. *Physical Review*, 36(5), pp. 823–841. DOI: <https://doi.org/10.1103/PhysRev.36.823>.

Vanherberghen, B. *et al.* (2013) *Classification of human natural killer cells based on migration behavior and cytotoxic response*. *Blood*, 121(8), pp. 1326–1334. DOI: <https://doi.org/10.1182/blood-2012-06-439851>.

Verron, Q. *et al.* (2021) *NK cells integrate signals over large areas when building immune synapses but require local stimuli for degranulation*. *Science Signaling*, 14(684), p. eabe2740. DOI: <https://doi.org/10.1126/scisignal.abe2740>.

Virtanen, P. *et al.* (2020) *SciPy 1.0: fundamental algorithms for scientific computing in Python*. *Nature Methods*, 17(3), pp. 261–272. DOI: <https://doi.org/10.1038/s41592-019-0686-2>.

Waskom, M.L. (2021) *seaborn: statistical data visualization*. *Journal of Open Source Software*, 6(60), p. 3021. DOI: <https://doi.org/10.21105/joss.03021>.

Weigelin, B. *et al.* (2021) *Cytotoxic T cells are able to efficiently eliminate cancer cells by additive cytotoxicity*. *Nature Communications*, 12, p. 5217. DOI: <https://doi.org/10.1038/s41467-021-25282-3>.

Wolf, N.K., Kissiov, D.U. and Raulet, D.H. (2023) *Roles of natural killer cells in immunity to cancer, and applications to immunotherapy*. *Nature Reviews. Immunology*, 23(2), pp. 90–105. DOI: <https://doi.org/10.1038/s41577-022-00732-1>.

Yang, G. et al. (2014) *Low-Dose Ionizing Radiation Induces Direct Activation of Natural Killer Cells and Provides a Novel Approach for Adoptive Cellular Immunotherapy*. *Cancer Biotherapy & Radiopharmaceuticals*, 29(10), pp. 428–434. DOI: <https://doi.org/10.1089/cbr.2014.1702>.

Zhou, X. et al. (2017) *Bystander cells enhance NK cytotoxic efficiency by reducing search time*. *Scientific Reports*, 7(1), p. 44357. DOI: <https://doi.org/10.1038/srep44357>.

Acknowledgements

I would like to express my heartfelt thanks to my family: mother, grandmother, and grandfather for their unwavering mental and financial supports throughout my college study.

I am deeply grateful to my supervisor, Dr. Rubén Pérez-Carrasco for his guidance and supervision. My sincere thanks also go to my day-to-day supervisor, Elephes Sung, for his patience and daily guidance.